Bello-Jurado, E.; Margarit Benavent, VJ.; Gallego-Sánchez, EM.; Schuetze, F.; Hengst, C.; Corma Canós, A.; Moliner Marin, M. (2020). Deactivation and regeneration studies on Pd-containing medium pore zeolites as passive NOx adsorbers (PNAs) in cold-start applications. Microporous and Mesoporous Materials. 302:1-10. https://doi.org/10.1016/j.micromeso.2020.110222

Deactivation and regeneration studies on Pd-containing medium pore zeolites as passive NOx adsorbers (PNAs) in cold-start applications

Estefanía Bello,[1] Vicente J. Margarit,[1] Eva M. Gallego,[1] Frank Schuetze,[2] Christoph Hengst,[2] Avelino Corma*[1], Manuel Moliner*[1]

[1] Instituto de Tecnología Química, Universitat Politècnica de València-Consejo Superior de Investigaciones Científicas, Avenida de los Naranjos s/n, 46022 València, Spain

[2] Umicore AG&Co. KG, Hanau-Wolfgang, 63457, Germany

*Corresponding authors: E-mail addresses: mmoliner@itq.upv.es; acorma@itq.upv.es

Abstract

Two Pd-containing medium pore zeolite frameworks, MFI and MWW, have been evaluated as passive NOx adsorbers (PNAs) in automotive applications. The NOx adsorption/desorption behavior of Pd-containing standard ZSM-5 and MCM-22 zeolites with analogous physico-chemical properties (Si/Al~10-12, 1%wt Pd, crystal size of ~200-300 nm), has been first studied. Pd/ZSM-5 shows better low-temperature NOx capacity than Pd/MCM-22 (0.83 and 0.55 µmol NOx/µmol Pd), but, in contrast, Pd/MCM-22 is able to desorb NOx at remarkable lower temperatures (~50°C fewer). In order to evaluate the influence of the textural properties of the MWW-type materials on the NOx adsorption/desorption behavior, a delaminated DS-ITQ-2 and nano-MCM-22, have also been prepared. The deactivation of the different Pd-containing medium pore zeolites and their posterior regeneration have been systematically studied by subjecting the samples to CO-ageing treatments at different temperatures (from 150 to 650°C) and hydrothermal treatments at 750°C, respectively. Pd/ZSM-5 is able to almost fully recovery the former NOx adsorption capacity, whereas Pd/MWW materials only recuperate half of their initial NOx adsorption capacity, fact that can be explained by the larger critical sizes of part of the agglomerated metal particles on the external surface of these materials.

Keywords

Medium-pore zeolites, nitrogen oxides (NOx), selective catalytic reduction (SCR), passive NOx adsorbers (NOx),

1.- Introduction

Nitrogen oxides (NOx) are harmful greenhouse gases, which are mainly responsible for the formation of smog and acid rain. Among many stationary and mobile sources, vehicles with diesel internal combustion engines are considered as the most significant NOx emitting source vehicles and, thus, many efforts have been devoted in the last 10 years to develop catalytic systems that allow meeting restrictive legislation on NOx emission limits.[1]

The selective catalytic reduction of NOx (NOx-SCR) using ammonia as reducing agent and Cu-containing small-pore zeolites as catalysts has been shown as very active and stable catalytic systems for these automotive applications,[2, 3] which adequately perform under driving conditions at temperatures comprised between 200 and 500°C.[4-6] However, the small pore Cu-zeolites give low activity for NOx-SCR at temperatures below 150°C, fact that occurs during the vehicle ignition and, then, results in a significant NOx release to the atmosphere during this "cold-start" period.[7]

Different research groups have recently reported the use of diverse Pd-containing zeolites as effective materials to trap NOx at low temperatures (below 100°C) and, once the system has reached higher temperatures (above 250°C), the NOx is released to allow their selective catalytic reduction with the Cu-based zeolite catalyst.[8-10] The Pd-zeolites act as passive NOx adsorbers (PNAs) in the exhaust gas after-treatment systems for automotive applications.[11, 12] Outstanding achievements have been reported in the last two years on the fundamental understanding of the structure-function relationships for NOx adsorption/desorption in Pd-supported zeolites.[10, 13] However, the highly-dynamic nature of the Pd species during the NOx adsorption/desorption cycles makes the selection and design of the zeolite support with the adequate physico-chemical properties very challenging for its application as active and stable PNA.[9, 10, 14]

In general, highly dispersed Pd species have preferentially been proposed as the responsible sites for the chemisorptive NOx adsorption at low temperature.[10, 15, 16] Nevertheless, since the Pd-zeolite materials are exposed to the very dynamic and harsh conditions during the NOx adsorption/desorption cycles, sometimes also including high-temperatures and presence of well-known metal-sintering reagents, such as CO and water, the initially dispersed Pd species tend to migrate and to agglomerate as PdO clusters or larger particles, significantly reducing their performance as PNAs after several adsorption cycles.[17-21] The initial metal redispersion along the zeolite crystals could be achievable again by properly subjecting the aged Pd-zeolites to

hydrothermal treatments with steam at high temperatures (i.e. 750°C), permitting to recover most of the former NOx adsorption capacity.[20, 22] It is worth noting that for an efficient metal redispersion through high-temperature hydrothermal treatments is mandatory that the agglomerated PdO particles in the aged Pd-zeolites do not exceed a critical size (i.e. above 20 nm), because otherwise it would be very difficult to mobilize and redistribute the Pd species.[20]

Regarding the influence of the framework structure, it has been noticed that the NOx desorption temperature (T_{des}) correlates with pore openings.[9, 10] Indeed, the required T_{des} increases as the pore opening decreases, with a considerably higher T_{des} for the small-pore Pd-SSZ-13 zeolite than for the medium-pore Pd-ZSM-5 when the NOx adsorption/desorption is carried out under realistic conditions (i.e. presence of water and CO in the feed).[10] The control of T_{des} is a major concern when designing an effective PNA material, because the adsorber must be mostly unfilled for successive low temperature NOx adsorption cycles. Therefore, the design of active and stable Pd-containing medium-pore zeolites should also facilitate the NOx release at intermediate temperatures, allowing operative consecutive NOx adsorption/desorption cycles.

The outstanding stability of dispersed subnanometric noble-metal species (i.e. Pt or Pd) within the pores/cavities of the medium pore ZSM-5 (MFI) [23-26] and MCM-22 (MWW) zeolites,[27, 28] even when these materials are subjected to severe redox treatments, has been recently reported in the literature. These materials show bi-directional medium-pore frameworks, but with very different topologies. On the one hand, the MFI framework shows a bi-directional interconnected 10-ring pore system with a straight channel running perpendicular to a sinusoidal channel, both with pore openings of 5.4-5.6 Å.[29] On the other hand, the MWW structure is formed by two independent pore systems, i.e., a 10-ring zig-zag channel with pore openings of 5.1x4.1 Å and 12-ring cavities of 7.1x 18.2 Å connected by 10-ring apertures (see Figure 1).[30] These particular crystalline structures, presenting interconnected medium pores or large cavities for MFI and MWW, respectively, have been proposed for preventing metal sintering under harsh redox conditions.[23, 26, 28]

If the MWW structure is deeply analyzed, it can be observed that its external surface shows the presence of separated “cups” by exposing half of the 12-ring cavities (see Figure 1),[31] which could allocate not only acid sites, but also could stabilize extra-framework metallic species.[32, 33] Therefore, the control of the physico-chemical properties in the MWW structure, and particularly the ratio between external surface “cups” and internal cavities, could be an important parameter not only to enhance the metal dispersion, but also its resistance against undesired sintering. In this

sense, the one-pot synthesis of highly-delaminated MWW-type materials, DS-ITQ-2 and MIT-1, with high external surface has been achieved by using surfactant-based templates,[34, 35] together with the nanocrystalline MCM-22 material, nanoMCM-22, with average particles of 60-80 nm by using simple cyclic ammonium cations as organic modifiers in the synthesis media.[36, 37]

Herein, we have considered two medium pore zeolite frameworks, MFI and MWW, to evaluate their NOx adsorprtion/desorption capacity for their potential use as PNAs in automotive applications. Standard ZSM-5 and MCM-22 zeolites, both presenting similar physico-chemical properties (Si/Al~10-12 and crystal size of ~200-300 nm), have been initially considered as supports to introduce ~1 wt% Pd content. The NOx adsorption/desorption behavior of these two Pd-containing materials has been carried out with and without CO in the feed. The achieved results reveal that the low temperature adsorption capacity of the Pd/ZSM-5 is higher than the observed for Pd/MCM-22, but, in contrast, the NOx desorption temperature for Pd/MCM-22 is considerably lower than for Pd/ZSM-5. Two additional MWW-related materials, nano-MCM-22 and DS-ITQ-2, both presenting smaller particle sizes and larger external surfaces than the standard MCM-22, have been synthesized to study if the low temperature NOx adsorption capacity could be enhanced compared to the classical MCM-22. The metal resistance against sintering for the different Pd-containing medium-pore materials has been evaluated under severe ageing treatments with CO at different temperatures (from 150 to 650°C). In general, the four medium-pore Pd/zeolites show important and similar deactivation profiles when they have been subjected to the CO ageing treatments at high temperatures (650°C). However, Pd/ZSM-5 shows a substantially higher NOx adsorption capacity recovery after subjecting the CO-aged materials to hydrothermal treatments at 750°C in air and steam compared to the different MWW-type materials.

2.- Experimental

2.1.- Catalyst preparation

MCM-22,[38] nano-MCM-22 [36, 37] and DS-ITQ-2 [34] were synthesized following the methods described in the literature, and ZSM-5 was obtained from Zeolyst International Inc. (CBV-2314). The above samples were ion-exchanged with a 2M NH_4NO_3 aqueous solution at 80°C for 2 hours (liquid/solid mass ratio ~ 10) to obtain their ammonium form. The solid samples were washed and recovered by filtration, and dried at 100°C for 2 hours.

Finally, 1 wt% palladium was incorporated within the above ammonium-based zeolites by metal-exchange using a 0.1 wt% aqueous solution of $Pd(NH_3)_4(NO_3)_2$ (Sigma-Aldrich). 1.0 g of the NH_4-zeolites was added to 40 g of the aqueous Pd solution, and the mixture was maintained under stirring at room temperature overnight. After this period, the mixture was filtered, washed with abundant water, and dried at 100°C in an oven for 1 hour. Afterwards, the prepared catalysts were calcined at 650°C (2°C/min) in flowing air for 4 hours.

2.2.- Characterization

Powder X-ray diffraction (PXRD) measurements were performed with a multisample Philips X'Pert diffractometer equipped with a graphite monochromator, operating at 40 kV and 35 mA, and using Cu Kα radiation (λ = 0,1542 nm).

Chemical analyses were carried out in a Varian 715-ES ICP-Optical Emission spectrometer, after solid dissolution in HNO_3/HCl/HF aqueous solution.

The morphology of the samples was studied by field emission scanning electron microscopy (FESEM) using a ZEISS Ultra-55 microscope and by field emission transmission electron microscopy (TEM) using a JEM 2100F microscope.

Nitrogen adsorption isotherms at -196°C were measured on a Micromeritics ASAP 2020 with a manometric adsorption analyzer to determinate the textural properties of the samples.

2.3.- NOx adsorption/desorption experiments

NOx adsorption experiments were conducted in a continuous-flow quartz reactor, wherein 100 mg of pelletized samples (between 200 and 600 microns) were loaded. The temperature of the catalyst bed was measured by a type-K thermocouple inserted into the reactor and placed right above the catalyst bed. The NOx concentration was measured using an nCLD8xx analyser (ECO PHYSICS).

Prior to the NOx storage testing at 100°C, the samples were pretreated at 500°C for 2 hours with a 500 mL/min feed containing 5%vol CO_2, 5%vol water and 10%vol O_2, balanced with N_2. Afterwards, the reactor was cooled down to 100°C by flowing the same feed, and, at this point, the feed was then switched to 60 ppm of NO, 0-60 ppm of CO (depending if CO is present or not), 5%vol CO_2, 5%vol water and 10%vol O_2, balanced with N_2 (flow rate ~500 mL/min). The mixture passed through

the reactor at 100°C for 30 min, and, later, the temperature was raised to 500°C at the ramping rate of 17°C/min.

The different Pd/zeolites were aged with CO for 13 hours (60 ppm CO balanced with N_2 at a flow rate of 500 mL/min) at three different temperatures: 150°C, 350°C and 650°C. After the CO-ageing treatments, the following NOx adsorption/desorption cycle was carried out without previous activation: 60 ppm of NO, 60 ppm of CO, 5%vol CO_2, 5%vol water and 10%vol O_2, balanced with N_2 (flow rate ~500 mL/min). The mixture was passed through the reactor at 100°C for 30 min, and, later, the temperature was raised to 500°C at the ramping rate of 17°C/min.

The CO-aged samples have been hydrothermally treated with a flow containing 10%vol O_2, 5%vol H_2O, balanced with N_2 at a flow rate of 500 mL/min, at 750°C for 13 hours to evaluate the metal redispersion on these materials. After the hydrothermal treatments, the following NOx adsorption/desorption cycle was carried: 60 ppm of NO, 60 ppm of CO, 5%vol CO_2, 5%vol water and 10%vol O_2, balanced with N_2 (flow rate ~500 mL/min). The mixture was passed through the reactor at 100°C for 30 min, and, later, the temperature was raised to 500°C at the ramping rate of 17°C/min.

3.- Results and Discussion

3.1.- Synthesis and characterization of the medium pore ZSM-5 and MWW-type zeolites

Standard medium-pore MCM-22 and ZSM-5 materials have been first selected to evaluate their low temperature NOx adsorption capacities. In the case of ZSM-5, a commercially available material provided by Zeolyst has been selected (see PXRD pattern in Figure 2), with a Si/Al molar ratio of ~10.4 (see Table 1) and average crystal sizes between ~0.3-0.6 μm (see ZSM-5_Fresh in Figure 3). The conventional MCM-22 has been prepared according to the recipe described in the literature.[38] The as-prepared MCM-22 (MCM-22_ap) shows the characteristic PXRD pattern of the layered MCM-22(P) precursor, which is transformed into the final MCM-22 material through topotatic condensation by calcination in air at 580°C (see MWW framework in Figure 1 and PXRD pattern of MCM-22_calc in Figure 2). The ICP analysis reveals a Si/Al molar ratio for the MCM-22 zeolite of ~11.9 (see Table 1), and FE-SEM images show a platelet crystal morphology with average crystal sizes of ~0.3 μm (see MCM-22_Fresh in Figure 3), both characterization being analogous to those measured for ZSM-5.

As stated in the introduction, the original layered nature of the MWW structure makes this material very interesting with unique properties that allows controlling their external surface area by simple layer exfoliation through post-synthetic [31] or one-pot synthesis procedures.[34, 35] Following these approaches, it is possible to decrease the number of MWW layers forming part of the final MWW crystals, affording in the ideal case a single MWW layer, which is the ITQ-2 zeolite.[31] This highly-delaminated ITQ-2 material would only show the presence of the external "cups" and the circular 10-ring channels, but it will not have internal supercavities (see Figure 1), which have been described as efficient metal-trapping cages.[27, 28] Thus, an interesting material would be the partially-delaminated DS-ITQ-2,[34] which is formed in average by crystals with few MWW-layers (between 2-5) and, consequently, combines large external surface with the presence of internal supercavities. The DS-ITQ-2 material has been prepared following the recent description in the literature,[34] using an amphiphilic surfactant-based template. The PXRD pattern of the as-prepared material indicates the formation of the MWW structure (see DS-ITQ-2_ap in Figure 2), but the remarkably lower intensity of the diffraction peaks would agree with the presence of less MWW layers per particle compared to the standard MCM-22. The delaminated nature of the DS-ITQ-2 is confirmed after calcination in air at 580°C by TEM (see Figure 4-left) and by N_2 adsorption, which demonstrates the higher measured external surface area for the DS-ITQ-2 zeolite compared to classical MCM-22 (214 and 83 m^2/g, respectively, see Table 1). ICP characterization exposes a Si/Al molar ratio of 10.9, which is similar to ZSM-5 and MCM-22 materials (see Table 1).

Besides the delaminated DS-ITQ-2 material, the MCM-22 zeolite has also recently been synthesized in its nanosized form using simple non-surfactant molecules.[36] Following this recipe, the as-prepared nano-MCM-22 zeolite shows the characteristic PXRD of the layered MWW(P) precursor, which is transformed to the MWW structure by calcination with air at 600°C (see PXRD patterns for the nano-MCM-22_ap and nano-MCM-22_calc, respectively, in Figure 2). The nano-sized MCM-22 shows an average crystal size of 60-80 nm (see TEM image in Figure 4-right), resulting in a considerable reduction of the x-y axes of the MWW crystals (see Figure 1). It is worth noting that x-y axes are those favoring the access to the internal supercavities and zig-zag 10-ring pores of the MWW structure, so their reduction would enhance the diffusion paths towards the inner MWW cavities and pores compared to the classical MCM-22 or the partially-delaminated DS-ITQ-2. The N_2 adsorption indicates an intermediate external surface area, 124 m^2/g, between classical MCM-22 and DS-ITQ-2 (83 and 214 m^2/g, respectively, see Table 1). The Si/Al molar ratio of the nano-MCM-22 is analogous to the other materials (~11.2, see Table 1).

Once all the zeolitic materials have been synthesized and properly characterized, ~1 wt% Pd has been introduced by cation exchange (see experimental section for details). Chemical analyses of the Pd-exchanged materials indicate the nominal presence of ~1.2 wt% Pd for all of them (see Table 1). Before proceeding to the NOx adsorption/desorption evaluation, the four Pd-containing materials were calcined at 650°C in air. After this high-temperature oxidation treatment, FE-SEM images of the four samples do not reveal the presence of large metal agglomeration on the external surface, suggesting a good initial metal dispersion along the zeolitc crystals (see FE-SEM images of the fresh samples in Figure 3). A deeper inspection of the initial metal dispersion along these materials has been carried out by STEM microscopy (see Figure 5). STEM images reveal the preferential formation of small nanoparticles with sizes below 2 nm for all materials, but, in addition, a small fraction of large metal particles with sizes between 2 to 5 nm are also observed on the external surface of the four zeolites (see Figure 5).

3.2.- NOx adsorption/desorption performance: Influence of CO in the feed

The Pd-containing standard ZSM-5 and MCM-22 materials have been first evaluated as PNAs for the low-temperature NOx adsorption/desorption. For starting, the NOx adsorption/desorption of both materials has been carried out using CO-free feeds as a simplified reaction model, because CO is a well-known poison for metallic active sites and, in addition, can form volatile metal-carbonyl species at high temperatures, which can promote the undesired metal sintering on the external surface of the zeolitic crystals.[39] Thus, the feed was fixed at ~500 mL/min, with 60 ppm of NO, 5%vol CO_2, 5%vol water and 10%vol O_2, balanced with N_2. The mixture was passed through 100 mg of each Pd/zeolite, maintaining first the reactor at 100°C for 30 min to evaluate their low-temperature NOx adsorption capacity. Afterwards, the temperature was raised to 500°C at the ramping rate of 17°C/min to evaluate their NOx desorption capacity for multiple PNA cycles.

As seen in Figure 6a, Pd/ZSM-5 shows a slightly better NOx-uptake at 100°C than Pd/MCM-22 (53 and 40 µmol NOx/g, respectively, see Table 2). The overall NOx adsorption can even be increased when raising the reactor temperature between 120-240°C, observing a second NOx-uptake for both materials (see Pd/ZSM-5 and Pd/MCM-22 in Figure 6a), and providing a total NOx adsorption of 77 and 59 µmol NOx/g for the Pd/ZSM-5 and Pd/MCM-22, respectively (see Table 2). If these values are normalized by the Pd content in the zeolitic PNAs, Pd/ZSM-5 and Pd/MCM-22 materials give ~0.68 and ~0.52 µmol NOx/µmol Pd (see Table 2). These materials, and in particular Pd/MCM-22,

are relatively distant from the ideal maximum NOx adsorption behavior for Pd-based zeolitic PNAs, which has been reported theoretically as ~1.0 μmol NOx/μmol Pd.[16] However, if the NOx desorption profile is analyzed for these two materials, it can clearly be observed that Pd/MCM-22 is able to desorb NOx at a remarkably lower temperature than Pd/ZSM-5 by a difference of 50°C (see Figure 6a).

If one takes into account that the preferred configuration by automotive industry for treating the NOx-containing exhausts inevitably includes CO in the gas mixture that passes through the PNAs, more realistic conditions to evaluate PNAs require the presence of CO in the feed.[14, 17, 21] Recent literature reports indicate that the presence of CO in the feed induces a positive effect on NOx adsorption at low temperatures, increasing notoriously the PNA capacity.[14, 17, 21] It has been proposed that CO helps to form a stable Pd(II)(CO)(NO) complex and, additionally, the role of CO is to protect Pd from getting poisoned by water.[13, 16] Thus, considering these previous results, the NOx adsorption/desorption capacity of Pd/ZSM-5 and Pd/MCM-22 has been evaluated following the same conditions than before, but now including 60 ppm of CO in the feed. As can be seen in Figure 6b, both materials increase their NOx adsorption uptake at 100°C when CO is present in the feed. Indeed, the measured NOx adsorption values at 100°C are 92 and 59 μmol NOx/g for Pd/ZSM-5 and Pd/MCM-22, respectively, which are 1.7 and 1.4-fold higher than without CO for the same PNAs (see Table 2). Moreover, the entire NOx species are adsorbed at 100°C when CO is present in the feed, being almost negligible the second NOx adsorption step observed at higher temperatures (i.e. 120-220°C, see Figure 6b), and which was very significant in the adsorption experiments without CO (see temperatures between 120-220°C in Figure 6a).

If the NOx desorption profile is evaluated when CO is present in the feed, a faster NOx release rate can be seen for Pd/MCM-22 as compared to that of Pd/ZSM-5 (by a difference of ~57°C, see Figure 6b). This trend was also observed above under CO-free conditions. The preliminary results obtained are very interesting because the improved NOx-desorption performance when using Pd/MCM-22, even under more realistic conditions with CO in the gases, suggests that the MWW-structure could be an attractive medium-pore zeolite for its application as PNA. At this point, we do not have a definitive explanation for this experimental observation, but a direct relationship between the zeolite structure and the NOx desorption temperature has been proposed in the literature.[9] More fundamental studies are required for fully understanding the role of the MWW-structure on facilitating the NOx desorption.

However, the limited NOx adsorption capacity of the conventional Pd/MCM-22 compared to Pd/ZSM-5, prompted us to evaluate alternative MWW-materials with improved diffusion pathways. The objective was to improve the low-temperature NOx adsorption while keeping the lower NOx desorption temperature achieved with this zeolite. In this sense, the highly-delaminated Pd/DS-ITQ-2 and the Pd/nano-MCM-22 zeolites, both with a more favorable diffusion path, were prepared (see previous section for synthesis and characterization details).[34, 36] The NOx adsorption/desorption capacity of these materials was directly evaluated with the presence of CO in the feed (see Pd/DS-ITQ-2 and Pd-nano-MCM-22 in Figure 6b). On the one hand, their NOx adsorption capacities at 100°C are analogous to the conventional Pd/MCM-22 zeolite, with values of ~55-59 μmol NOx/g (see Table 2), corresponding to ~0.55 μmol NOx/μmol Pd. On the other hand, the NOx desorption profiles of the different Pd-containing MWW-type materials maintain the remarkably lower temperature (~383-395°C) compared to the Pd-ZSM-5 (~449°C, see Table 2), being slightly lower the NOx release temperature for the Pd-nano-MCM-22 zeolite (~383°C, see Table 2) than for conventional Pd-MCM-22 and DS-ITQ-2 (~392-395°C, see Table 2).

These results allow concluding that the NOx adsorption capacity using MWW-type PNAs could not be improved by just controlling their textural properties, at least when evaluated under fresh conditions. Nevertheless, it has been clearly demonstrated here that the MWW-type materials require lower NOx desorption temperatures compared to conventional Pd/ZSM-5 zeolite. At this point, and in order to improve the NOx adsorption capacity of the MWW-type materials, other physico-chemical parameters should be considered in these materials. We are now intensively studying the effect of the Al control distribution along the MWW-cavities and/or circular 10-ring pores, since the different stabilization of the Pd species along diverse crystallographic positions could have a dramatic impact on the overall NOx adsorption behaviour.[40]

3.3.- Resistance to deactivation: Ageing treatments with CO at different temperatures

The major deactivation factor for Pd-containing zeolites as PNAs is the undesired Pd sintering in presence of reducing gases, such as CO, which irremediable causes the decrease of the low-temperature NOx adsorption capacity of these materials.[18] This CO-mediated PNA deactivation mostly occurs by the formation of mobile Pd-carbonyl complexes that preferentially results in the metal sintering on the external surface of the zeolite crystals.[18] Considering this, the evaluation of the deactivation profiles of the medium-pore Pd/ZSM-5 and Pd/MWW-type zeolites has been

proposed by exposing these PNA materials to the reducing agent CO at different temperatures. To proceed with the ageing treatments, 500 mL/min of a CO-containing mixture (60 ppm CO balanced with N_2) was passed through 100 mg of each Pd/zeolite for 13 hours at the requested temperature (150, 350 and 650°C). After the CO-ageing treatments, the NOx adsorption/desorption cycle described above with CO in the feed has been carried out to evaluate the PNA capacity of the aged samples in comparison to their fresh counterparts.

The NOx adsorption capacity of the conventional Pd/ZSM-5 and Pd/MCM-22 zeolites shows a progressive decrease as the ageing temperature is increased from 150 to 650°C (see Figures 7a and 7b, respectively). The total NOx adsorption capacity loss is similar for both materials, ranging from ~20-30% to ~80-90% when the CO ageing treatment was carried out from 150 to 650°C, respectively (see Table 3). The analogous deactivation profiles of both medium-pore zeolites would suggest that the formation of volatile Pd-carbonyl complexes at a given ageing temperature would be comparable for Pd/ZSM-5 and Pd/MCM-22, regardless their different framework topologies, resulting in an extensive metal sintering on the external surface of the aged crystals. In fact, when the CO-aged Pd/ZSM-5 and Pd/MCM-22 materials have been characterized by FE-SEM, the metal sintering on the external surface of the crystals can be observed, being this sintering more extensive on the samples treated at higher temperatures (see for instance Pd/ZSM-5_CO350 and Pd/ZSM-5_CO650 in Figure 8).

To evaluate the average particle size of the metal agglomerates, the CO-aged samples at 650°C have been characterized by STEM microscopy. The aged Pd/ZSM-5 shows the superior presence of small nanoparticles with average sizes below ~4 nm together with the formation of larger aggregates with sizes between 10-15 nm (see Pd/ZSM-5_CO650 in Figure 9). In contrast, the aged Pd/MCM-22 presents the preferential formation of larger aggregates of ~20 nm and less smaller particles with sizes of 5 nm (see Pd/MCM-22_CO650 in Figure 9). Despite the deactivation profile being similar for both materials, the existence of larger metal agglomerates along the external surface of the Pd/MCM-22 zeolite could impact the regeneration of the aged materials for their continuous use as efficient PNAs.

The CO-ageing treatment at 650°C has also been carried out on the Pd/MWW-type materials synthesized with larger external surface area (Pd/nano-MCM-22 and Pd/DS-ITQ-2) in order to compare with conventional Pd/ZSM-5 and Pd/MCM-22. The measured NOx adsorption capacity loss

for both high external surface area Pd/MWW-related materials approaches ~80-90% (see Table 3), which is analogous to those measured using CO-aged conventional Pd/zeolites. STEM images on the CO-aged Pd/MWW-type materials show a dual distribution particle sizes of ~3-5 and ~15 nm for Pd/nano-MCM-22 (see Figure 9), similarly to those observed for Pd/MCM-22, whereas DS-ITQ-2 presents the preferential formation of large metallic particles with average crystals sizes between 15 and 25 nm (see Figure 9). Despite there is not a definitive explanation for the different metal sintering among the Pd/MWW materials, the remarkably lower micropore volume measured for Pd/DS-ITQ-2 material as consequence of the very few MWW layers conforming its crystals, could be a plausible description that would justify lower diffusional limitations to the metal-carbonyl complexes towards the external surface.

3.4.- PNAs regeneration: Hydrothermal treatments at high temperature with steam

The hydrothermal treatment (HT) with air and steam at 750°C has been described as an efficient method to study the regeneration of aged Pd/zeolites, allowing the redistribution of agglomerated Pd particles within the zeolite frameworks.[19, 22] Thus, the different aged medium-pore Pd/zeolites have been treated with a flow containing oxygen and water (10 vol% O_2 and 5 vol% H_2O, balanced with N_2), at 750°C for 13 hours.

When the PNAs regeneration is studied with the conventional Pd/ZSM-5 and Pd/MCM-22 samples, it can be observed that the Pd/ZSM-5 shows an improved regeneration of the initial NOx adsorption capacity with respect to Pd/MCM-22 (see Figure 10 and Table 4). In fact, it appears from the experimental data that the Pd/ZSM-5 material is able to fully recover the initial NOx adsorption capacity of the fresh material after CO-ageing at 350°C (see Pd/ZSM-5_CO350_HT750 in Table 4), and almost 80% of the former NOx adsorption capacity after CO-ageing at 650°C (see Pd/ZSM-5_CO650_HT750 in Table 4). In contrast, the conventional Pd/MCM-22 zeolite only recovers ~50% of its initial NOx adsorption capacity (see Pd/MCM-22_CO650_HT750 in Table 4). The limited regeneration ability of the Pd/MCM-22 could be related to the formation of larger metal agglomerates (~15-20 nm) during the CO-ageing treatments, and this critical size does not allow an effective particle break-up and metal redispersion. Indeed, large metal nanoparticles are still observed on the external surface of the Pd/MCM-22 after the HT treatments with air and steam at 750°C (see Pd/MCM-22_CO650_HT750 in Figure 11).

The Pd/MWW-type zeolites with improved textural properties have also been hydrothermally treated at 750°C. As seen in Table 4, the Pd/nano-MCM-22 zeolite recovers ~50% of the initial NOx adsorption capacity, whereas the Pd/DS-ITQ-2 zeolite recuperates only ~20% of its former NOx adsorption capacity. The different metal sintering during the CO-ageing treatment should be the main reason explaining these substantial differences. In the case of the aged Pd/nano-MCM-22_CO650, a bimodal metal distribution was shown (see Figure 9) and, thus, the redispersion of the smaller particles during the hydrothermal treatment at 750°C was possible (see Pd/nano-MCM-22_CO650_HT750 in Figure 11). On the contrary, the aged Pd/DS-ITQ-2 presented preferentially the formation of very large Pd particles on the external surface and, consequently, these massive particles have been barely redispersed during the hydrothermal treatment (see Pd/nano-MCM-22_CO650_HT750 in Figure 11), explaining the very low NOx adsorption capacity of this material after the ageing/redispersion treatments.

The combination of CO-ageing and HT-dispersion treatments at different temperatures could be considered as an effective accelerated ageing treatment to evaluate the kinetics behind the sintering/redispersion of metallic species. An optimized CO-ageing/hydrothermal treatment could shed light to estimate the ideal moment to proceed to regenerate a PNA under realistic conditions after a particular number of adsorption/desorption cycles and lower regeneration temperatures.

4.- Conclusions

Two different Pd-containing medium-pore zeolites, Pd/ZSM-5 and Pd/MCM-22, have been evaluated as PNA materials for the efficient low-temperature NOx adsorption/desorption as complement to SCR-NOx systems. Preliminary results have shown that Pd/ZSM-5 presents higher low-temperature NOx capacity than Pd/MCM-22 (0.83 and 0.55 µmol NOx/µmol Pd), but, interestingly, Pd/MCM-22 shows a remarkably lower NOx desorption temperature than Pd/ZSM-5 (~50°C fewer). Related MWW-materials, nano-MCM-22 and DS-ITQ-2, have been synthesized with enhanced textural properties to attempt the improvement of the low-temperature NOx uptake. The Pd-containing medium pore zeolites have been aged with CO at different temperatures (from 150 to 650°C) to evaluate their resistance against deactivation. After these CO-treatments, similar deactivation profiles in terms of NOx adsorption capacity for the entire Pd/containing medium-pore zeolites are observed, but the formation of different metal agglomerates are revealed depending on the zeolite support, being, in general, larger for MWW-type materials. The regeneration of the

aged Pd/zeolites following a hydrothermal treatment with air and steam at high temperature (i.e. 750°C), has resulted in an almost fully recovery of the former NOx adsorption capacity for the Pd/ZSM-5, whereas Pd/MCM-22 and Pd/nano-MCM-22 materials only recuperate half of their initial NOx adsorption capacity. The large critical size achieved for part of the agglomerated metal particles on the external surface of the MWW-related materials does not allow the proper metal redispersion. Additional synthesis rationalization attempting to populate the Al species along the MWW structure in different crystallographic positions could induce improvements on metal-resistance against deactivation for Pd/MWW-type materials.

Acknowledgements

This work has been supported by Umicore and by the Spanish Government through SEV-2016-0683 and RTI2018-101033-B-I00 (MCIU/AEI/FEDER, UE). E.B. acknowledges the Spanish Government-MCIU for a FPI scholarship. E.M.G. acknowledges “La Caixa - Severo Ochoa” International PhD Fellowships (call 2015). We thank I. Millet for technical assistance. The Electron Microscopy Service of the UPV is acknowledged for their help in sample characterization.

Figure 1: Scheme of the MWW framework

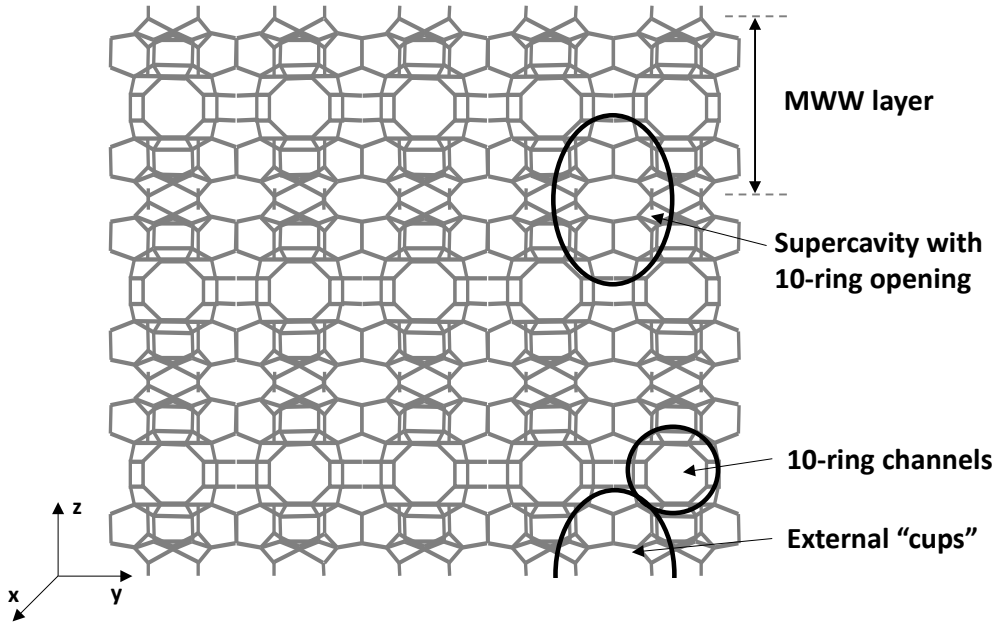

Figure 2: PXRD patterns of the different medium-pore zeolites

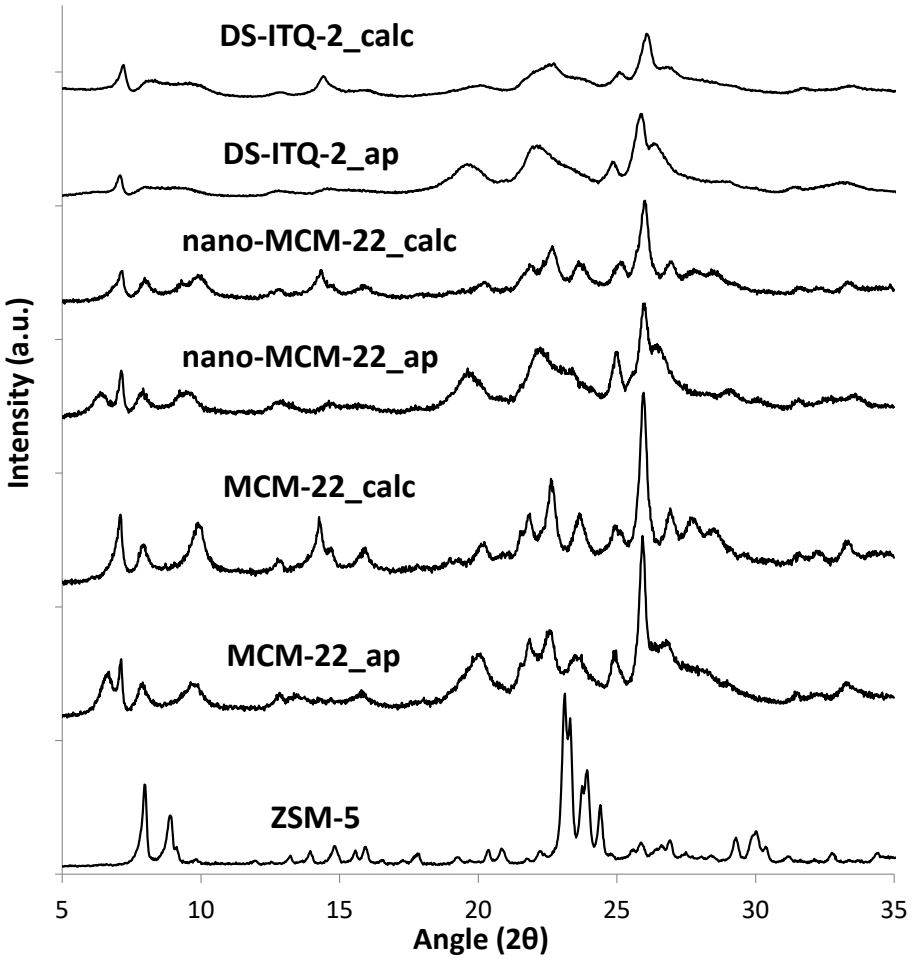

Figure 3: FE-SEM images of the fresh Pd/zeolite samples

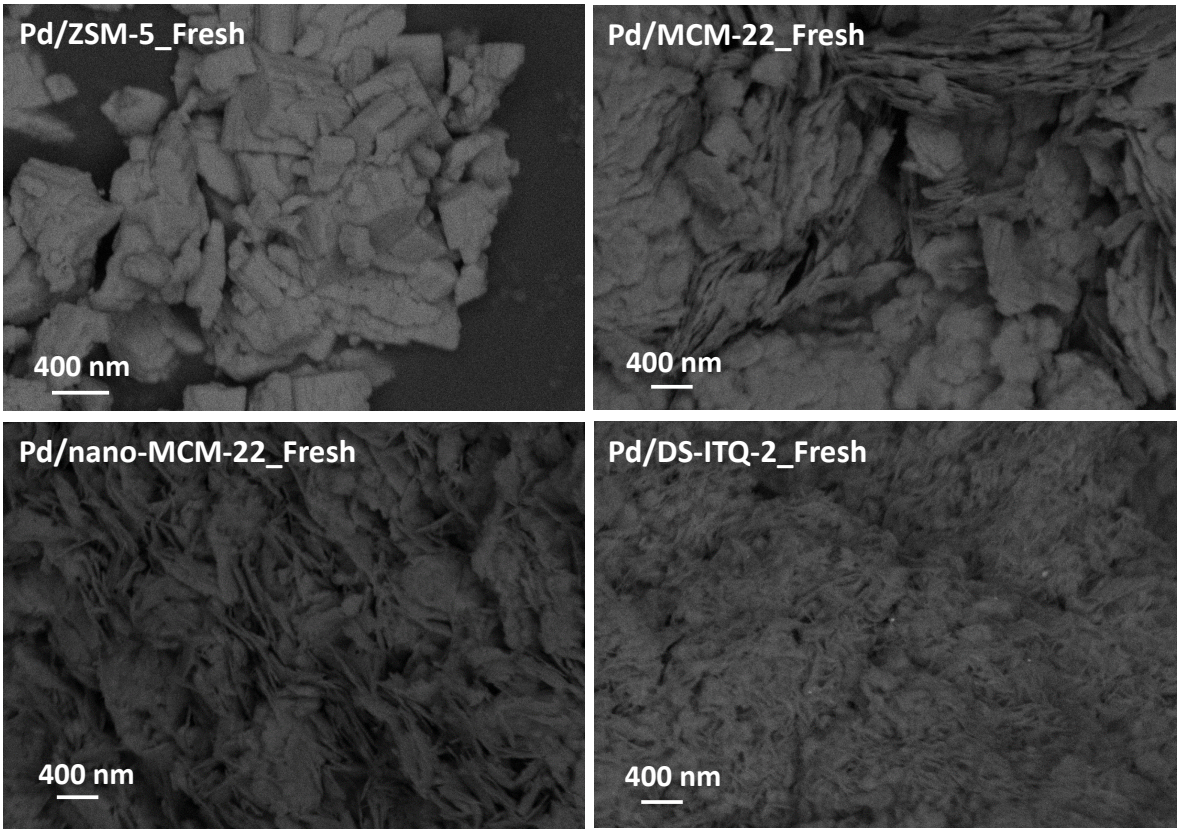

Figure 4: HRTEM images of the DS-ITQ-2 (left) and nano-MCM-22 (right)

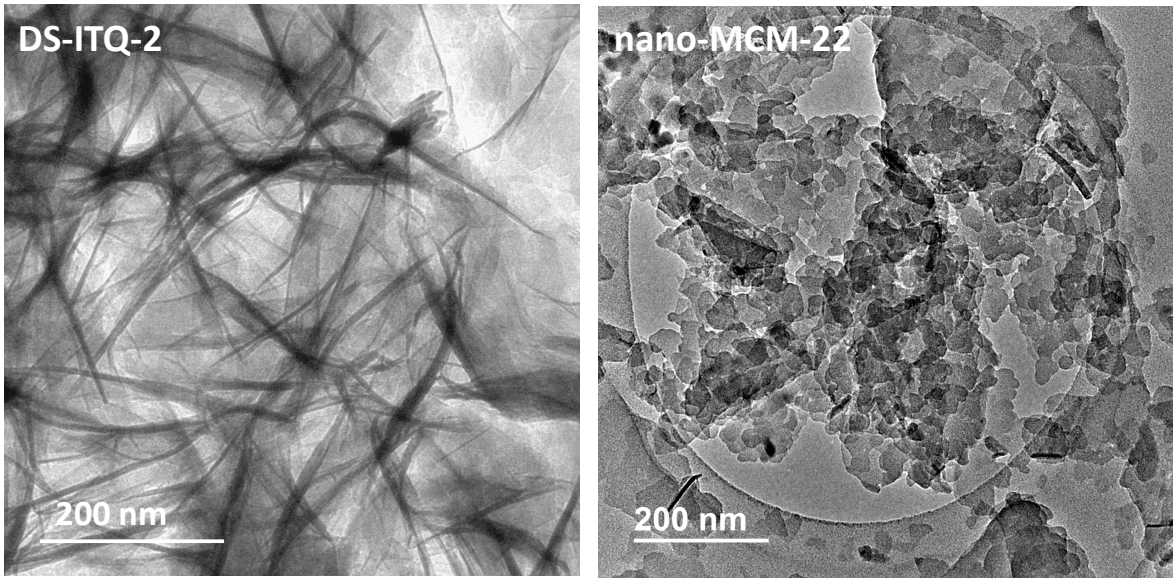

Figure 5: STEM images of the fresh Pd/zeolite samples

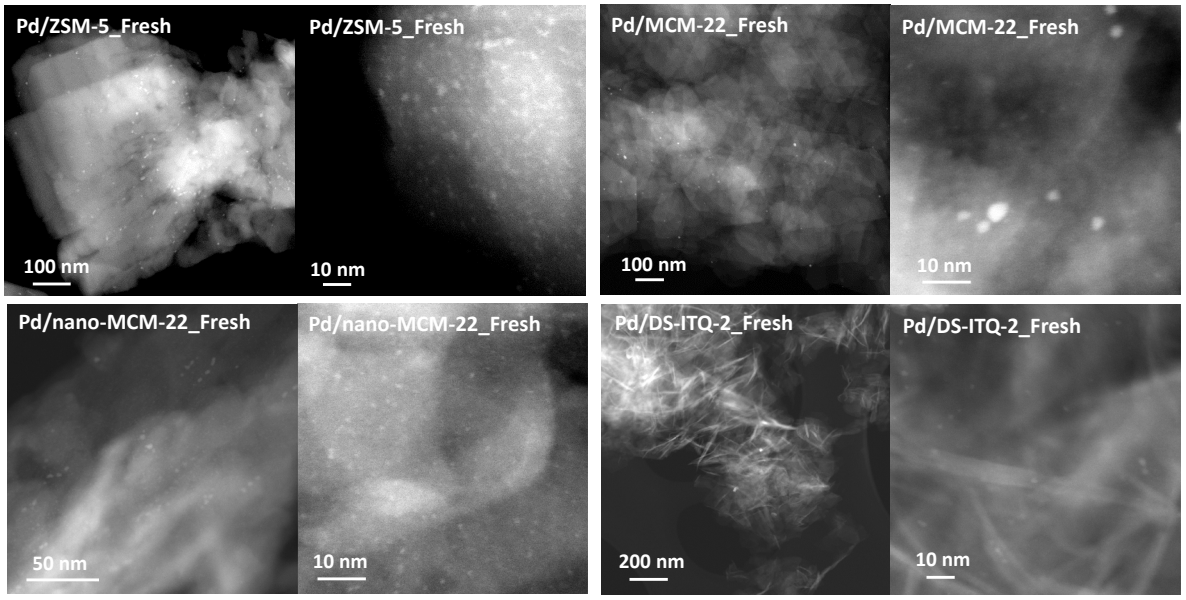

Figure 6: (a) NOx adsorption/desorption behavior of the fresh Pd/zeolites without CO in the feed. (b) NOx adsorption/desorption behavior of the fresh Pd/zeolites with CO in the feed. Reaction conditions: 500 ml/min (60 ppm NO, 0-60 ppm CO, 5%vol CO_2, 10%vol O_2, 5%vol H_2O, and N_2)

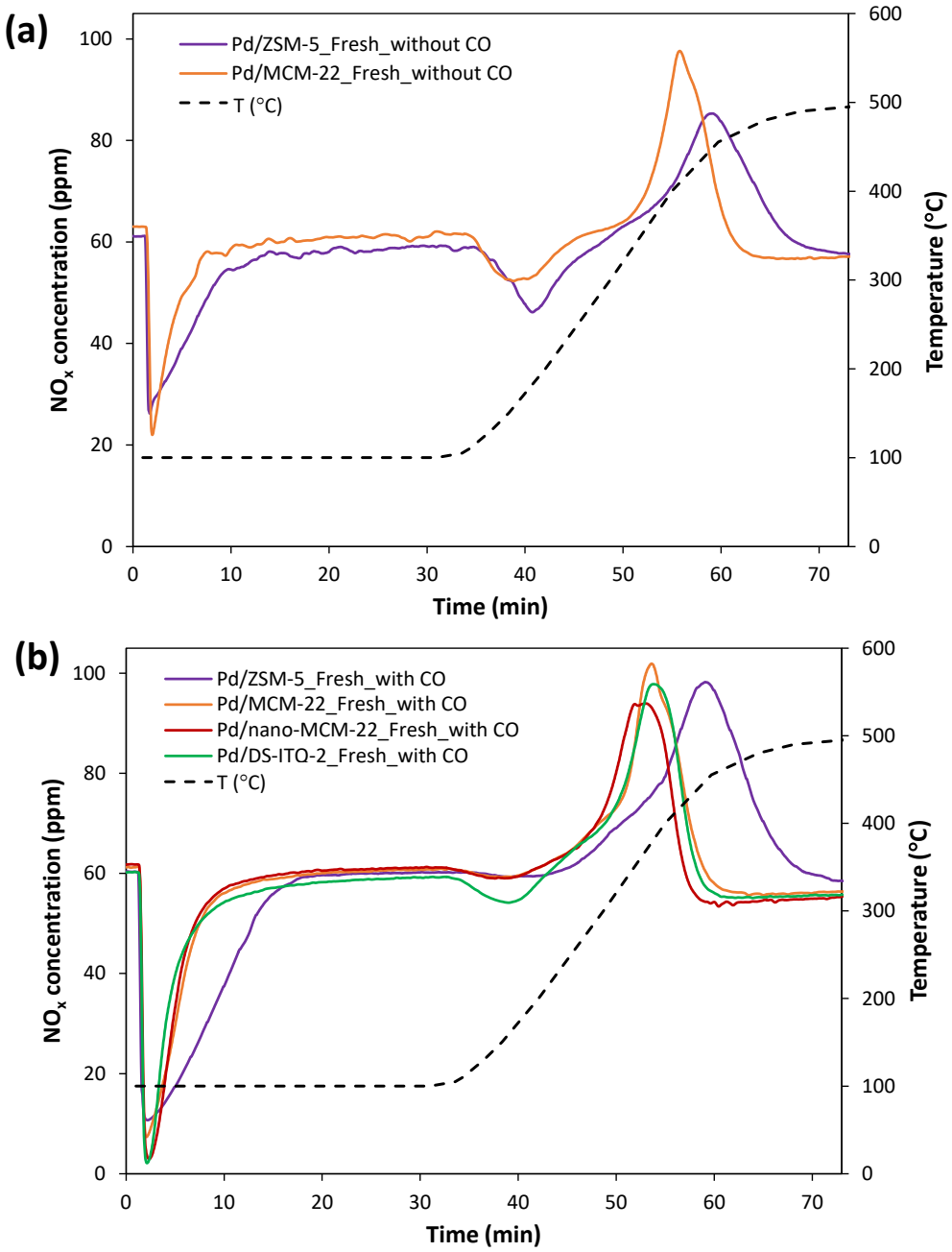

Figure 7: NOx adsorption/desorption behavior of Pd/ZSM-5 (a), Pd/MCM-22 (b), Pd/nanoMCM-22 (c) and Pd/DS-ITQ-2 (d) after being aged with CO at different temperatures. Reaction conditions: 500 ml/min (60 ppm NO, 60 ppm CO, 5%vol CO_2, 10%vol O_2, 5%vol H_2O, and N_2)

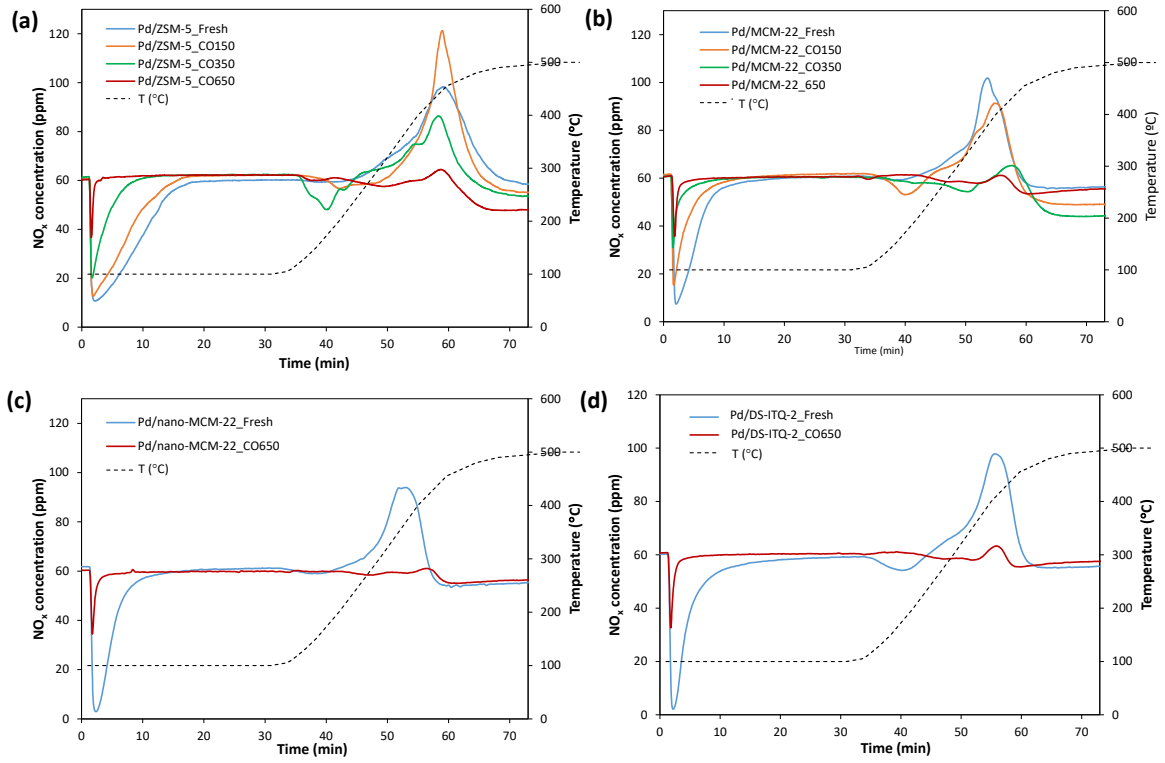

Figure 8: FE-SEM images of the Pd/zeolites after being aged with CO at 350 or 650°C.

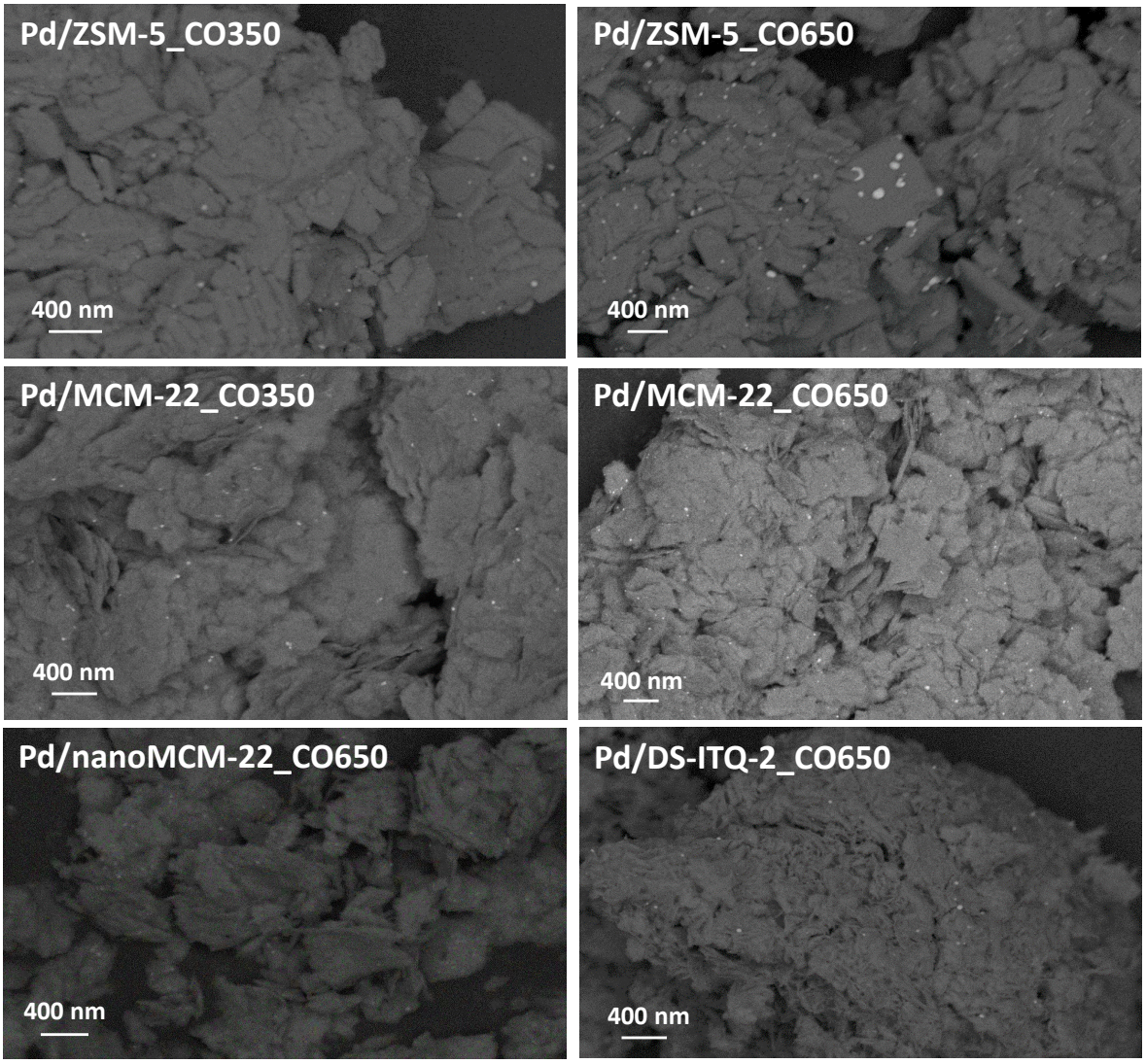

Figure 9: STEM images of the Pd/zeolites after being aged with CO at 650°C.

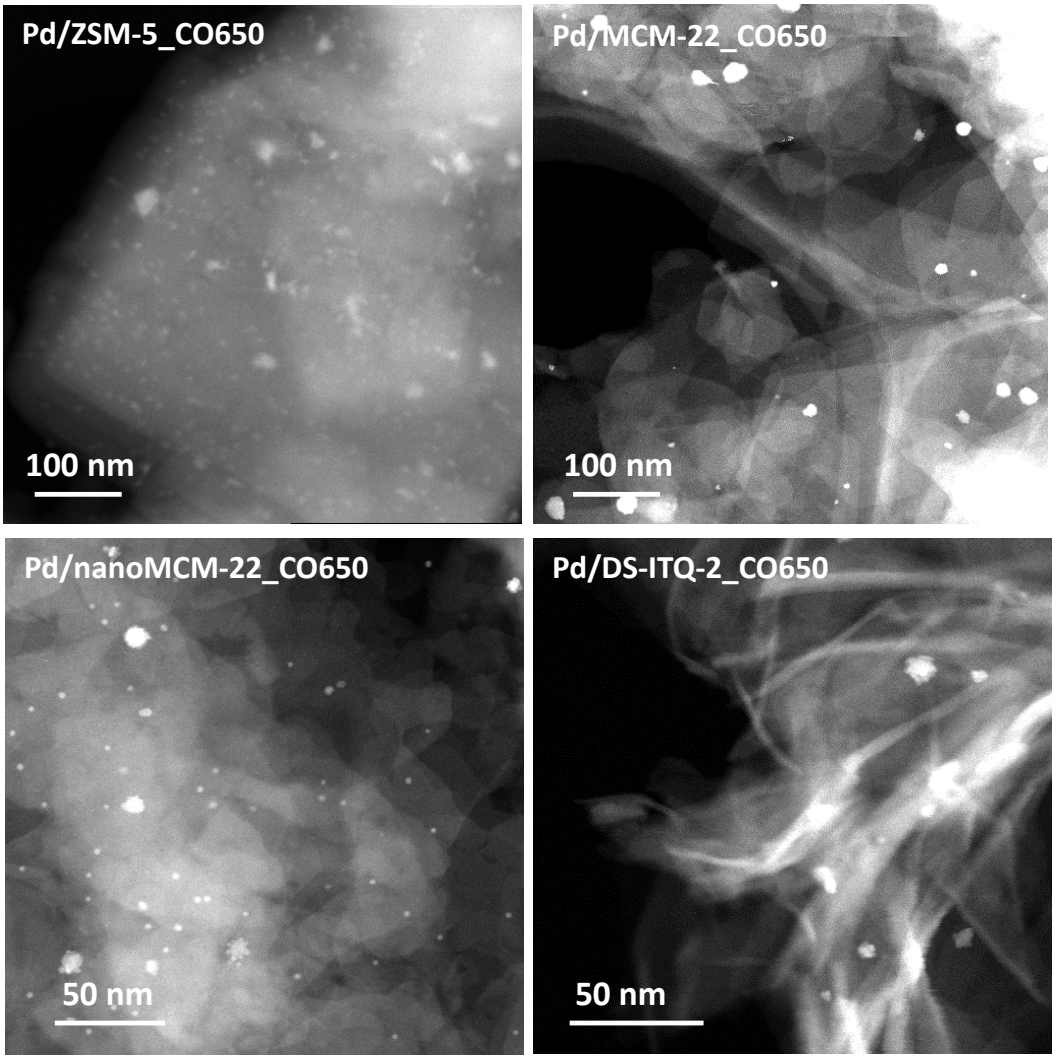

Figure 10: NOx adsorption/desorption behavior of the CO-aged Pd/ZSM-5 (a), Pd/MCM-22 (b), Pd/nanoMCM-22 (c) and Pd/DS-ITQ-2 (d) after being hydrothermally treated with air and steam at 750°C. Reaction conditions: 500 ml/min (60 ppm NO, 60 ppm CO, 5%vol CO_2, 10%vol O_2, 5%vol H_2O, and N_2)

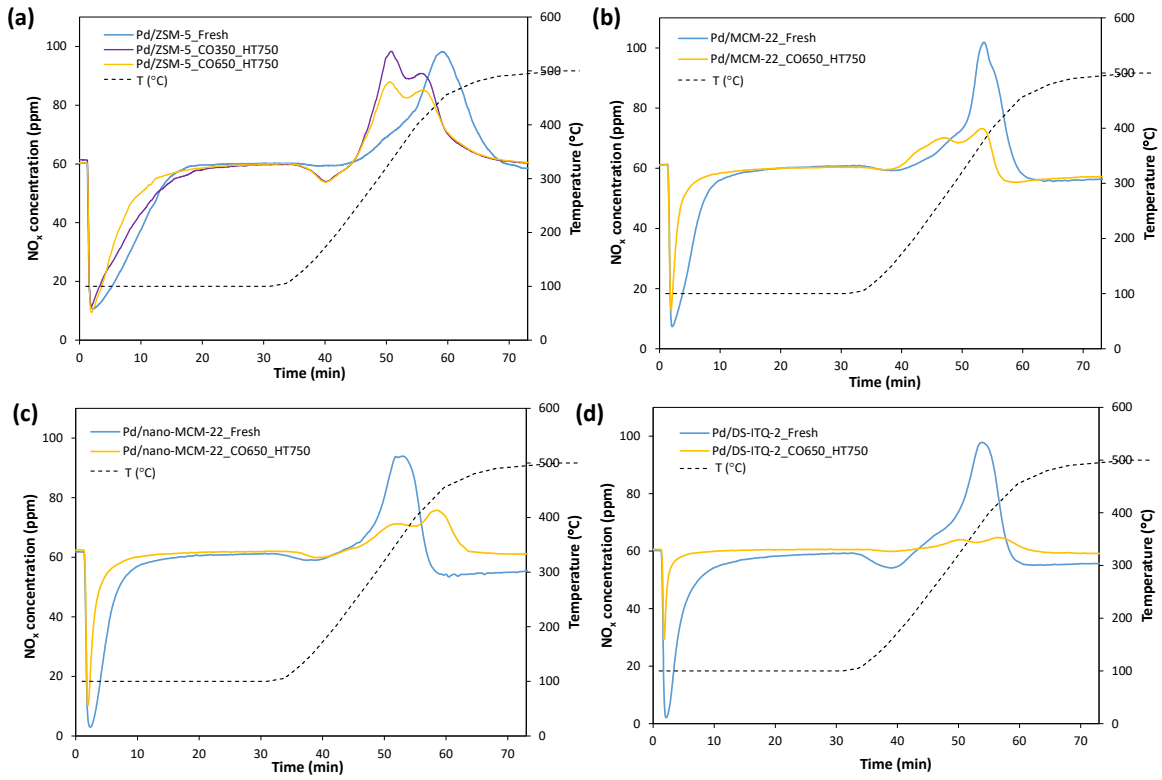

Figure 11: STEM images of the CO-aged Pd/zeolites after being hydrothermally treated with air and steam at 750°C.

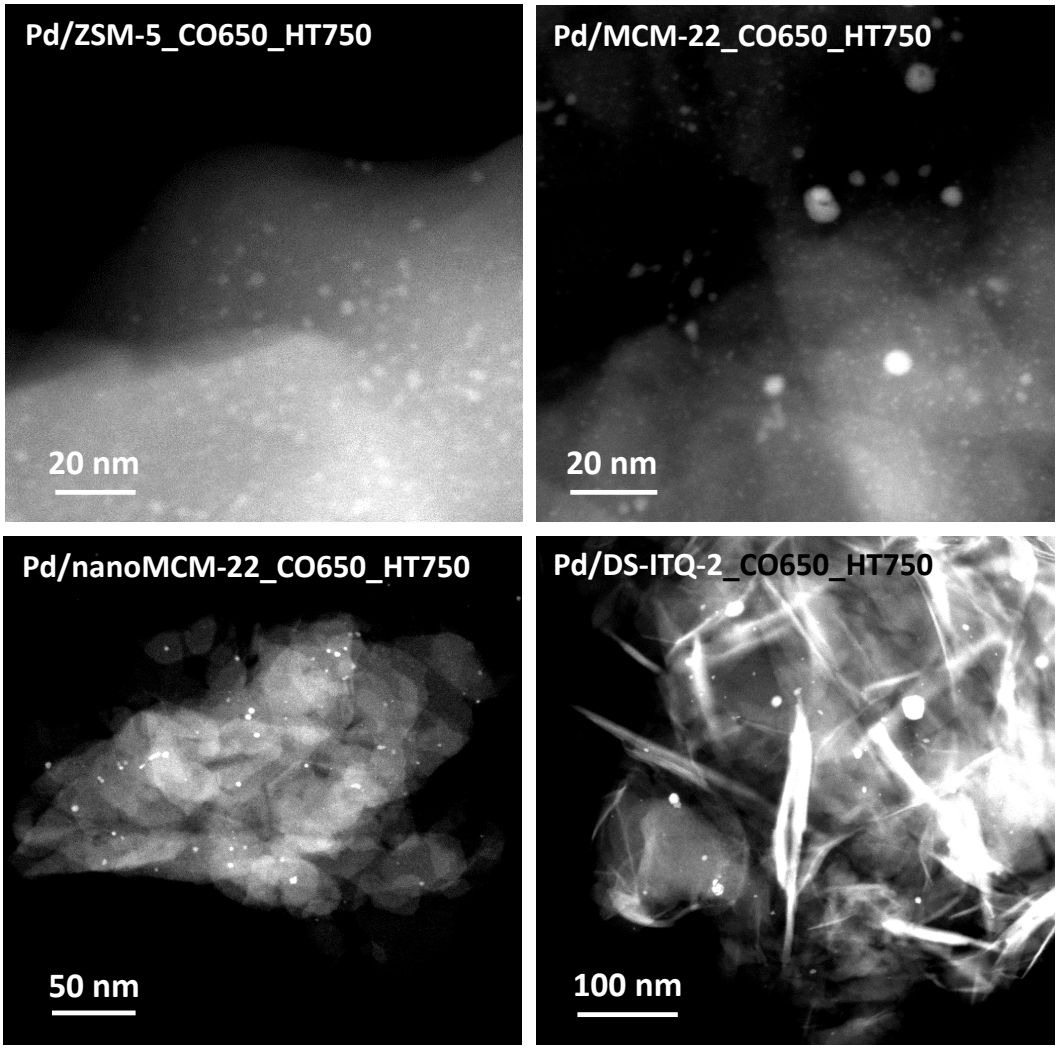

Table 1: Chemical analyses and textural properties of the different medium-pore Pd-containing zeolites

Sample	BET surface area (m^2/g)	Ext. surf. area (m^2/g)	Microp. Volume (cm^3/g)	Si/Al	Pd (wt%)
ZSM-5	370	22	0.16	10.4	1.18
MCM-22	457	83	0.19	11.9	1.22
nano-MCM-22	483	124	0.17	11.2	1.20
DS-ITQ-2	525	214	0.15	10.9	1.22

Table 2: Measured NOx adsorption/desorption for the different materials fresh materials without and with CO in the feed (500 ml/min (60 ppm NO, 0-60 ppm CO, 5%vol CO_2, 10%vol O_2, 5%vol H_2O, and N_2)

Sample	µmol NOx/g (100°C)	µmol NOx/g (total)	µmol NOx total/µmol Pd	Temp. Desorp. (°C)
Pd/ZSM-5_fresh (without CO)	53	77	0.68	448
Pd/ZSM-5_fresh (with CO)	92	93	0.83	449
Pd/MCM-22_fresh (without CO)	40	59	0.52	398
Pd/MCM-22_fresh (with CO)	59	62	0.55	392
Pd/nano-MCM-22 (with CO)	57	62	0.55	383
Pd/DS-ITQ-2 (with CO)	55	64	0.56	395

Table 3: Measured NOx adsorption/desorption for the different materials Pd-containing materials after being aged with CO at different temperatures

Sample	µmol NOx/g (100°C)	µmol NOx/g (total)	µmol NOx total/µmol Pd	Temp. Desorp. (°C)	Total NOx Adsorp. Capacity Loss (%)
Pd/ZSM-5_CO150	66	71	0.63	446	24
Pd/ZSM-5_CO350	26	39	0.34	440	59
Pd/ZSM-5_CO650	3	7	0.06	455	93
Pd/MCM-22_CO150	32	41	0.37	411	32
Pd/MCM-22_CO350	13	27	0.23	430	58
Pd/MCM-22_CO650	11	12	0.10	430	81
Pd/nano-MCM-22_CO650	9	13	0.11	414	80
Pd/DS-ITQ-2_CO650	9	10	0.07	420	87

Table 4: Measured NOx adsorption/desorption for the different materials CO-aged Pd-containing materials after being hydrothermally treated with air and steam at 750°C

Sample	µmol NOx/g (100°C)	µmol NOx/g (total)	µmol NOx total/µmol Pd	Temp. Desorp. (°C)	Total NOx Adsorp. Capacity Recovery (%)
Pd/ZSM-5_CO350_HT750	88	99	0.88	332/410	106
Pd/ZSM-5_CO650_HT750	66	72	0.64	329/410	77
Pd/MCM-22_CO650_HT750	27	29	0.26	265/385	47
Pd/nano-MCM-22_CO650_HT750	27	31	0.27	331/445	49
Pd/DS-ITQ-2_CO650_HT750	9	10	0.09	321/423	16

References:

[1] K. Skalska, J.S. Miller, S. Ledakowicz, Trends in NOx abatement: A review, Sci. Total Env., 408 (2010) 3976-3989.
[2] A.M. Beale, F. Gao, I. Lezcano-Gonzalez, C.H.F. Peden, J. Szanyi, Recent advances in automotive catalysis for NOx emission control by small-pore microporous materials, Chem. Soc. Rev., 44 (2015) 7371-7405.
[3] M. Moliner, C. Martínez, A. Corma, Synthesis Strategies for Preparing Useful Small Pore Zeolites and Zeotypes for Gas Separations and Catalysis, Chem. Mater., 26 (2014) 246-258.
[4] I. Bull, R.S. Boorse, W.M. Jaglowski, G.S. Koermer, A. Moini, J.A. Patchett, W.M. Xue, P. Burk, J.C. Dettling, M.T. Caudle, Copper CHA Zeolinte Catalysts, US20080226545, (2008).
[5] D.W. Fickel, E. D'Addio, J.A. Lauterbach, R.F. Lobo, The ammonia selective catalytic reduction activity of copper-exchanged small-pore zeolites, Appl. Catal. B, 102 (2011) 441-448.
[6] M. Moliner, C. Franch, E. Palomares, M. Grill, A. Corma, Cu–SSZ-39, an active and hydrothermally stable catalyst for the selective catalytic reduction of NOx, Chem. Commun., 48 (2012) 8264-8266.
[7] V. Schmeisser, M. Weibel, L. Sebastian Hernando, I. Nova, E. Tronconi, M.P. Ruggeri, Cold Start Effect Phenomena over Zeolite SCR Catalysts for Exhaust Gas Aftertreatment, SAE Int. J. Commer. Veh., 6 (2013) 190-199.
[8] R.R. Rajaram, H.Y. Chen, D. Liu, Passive NOx adsorber US20150158019, (2015).
[9] H.Y. Chen, J.E. Collier, D. Liu, L. Mantarosie, D. Durán-Martín, V. Novák, R.R. Rajaram, D. Thompsett, Low Temperature NO Storage of Zeolite Supported Pd for Low Temperature Diesel Engine Emission Control, Catal. Lett., 146 (2016) 1706-1711.
[10] Y. Zheng, L. Kovarik, M.H. Engelhard, Y. Wang, Y. Wang, F. Gao, J. Szanyi, Low-Temperature Pd/Zeolite Passive NOx Adsorbers: Structure, Performance, and Adsorption Chemistry, J. Phys. Chem. C, 121 (2017) 15793-15803.
[11] M. Moliner, A. Corma, From metal-supported oxides to well-defined metal site zeolites: the next generation of passive NOx adsorbers for low-temperature control of emissions from diesel engines React. Chem. Eng., 4 (2019) 223-234.
[12] Y. Gu, W.S. Epling, Passive NOx adsorber: An overview of catalyst performance and reaction chemistry, Appl. Catal. A, 570 (2019) 1-14.
[13] K. Khivantsev, F. Gao, L. Kovarik, Y. Wang, J. Szanyi, Molecular Level Understanding of How Oxygen and Carbon Monoxide Improve NOx Storage in Palladium/SSZ-13 Passive NOx Adsorbers: The Role of NO+ and Pd(II)(CO)(NO) Species, J. Phys. Chem. C, 122 (2018) 10820-10827.
[14] K. Khivantsev, N.R. Jaegers, L. Kovarik, J.Z. Hu, F. Gao, Y. Wang, J. Szanyi, Palladium/Zeolite Low Temperature Passive NOx Adsorbers (PNA):Structure-Adsorption Property Relationships for HydrothermallyAged PNA Materials, Emiss. Control Sci. Technol., DOI: 10.1007/s40825-019-00139-w (2019).
[15] J. Lee, Y.S. Ryou, S.J. Cho, H. Lee, C.H. Kim, D.H. Kim, Investigation of the active sites and optimum Pd/Al of Pd/ZSM–5 passive NO adsorbers for the cold-start application: Evidence of isolated-Pd species obtained after a high-temperature thermal treatment, Appl. Catal. B, 226 (2018) 71-82.
[16] K. Khivantsev, N.R. Jaegers, L. Kovarik, J.C. Hanson, F. Tao, Y. Tang, X. Zhang, I.Z. Koleva, H.A. Aleksandrov, G.N. Vayssilov, Y. Wang, F. Gao, J. Szanyi, Achieving Atomic Dispersion of Highly Loaded Transition Metals in Small-Pore Zeolite SSZ-13: High-Capacity and High-Efficiency Low-Temperature CO and Passive NOx Adsorbers, Angew. Chem. Int. Ed., 57 (2018) 16672-16677.
[17] A. Vu, J. Luo, J. Li, W.S. Epling, Effects of CO on Pd/BEA Passive NOx Adsorbers, Catal. Lett., 147 (2017) 745-750.

[18] Y.S. Ryou, J. Lee, Y. Kim, S. Hwang, H. Lee, C.H. Kim, D.H. Kim, Effect of reduction treatments (H2 vs. CO) on the NO adsorption ability and the physicochemical properties of Pd/SSZ-13 passive NOx adsorber for cold start application, Appl. Catal. A, 569 (2019) 28-34.
[19] Y.S. Ryou, J. Lee, H. Lee, C.H. Kim, D.H. Kim, Effect of various activation conditions on the low temperature NO adsorption performance of Pd/SSZ-13 passive NOx adsorber, Catal. Today, 320 (2019) 175-180.
[20] Y. Gu, R.P. Zelinsky, Y.R. Chen, W.S. Epling, Investigation of an irreversible NOx storage degradation Mode on a Pd/BEA passive NOx adsorber, Appl. Catal. B, 258 (2019) 118032.
[21] K. Khivantsev, N.R. Jaegers, L. Kovarik, S. Prodinger, M.A. Derewinski, Y. Wang, F. Gao, J. Szanyi, Palladium/Beta zeolite passive NOx adsorbers (PNA): Clarification of PNA chemistry and the effects of CO and zeolite crystallite size on PNA performance, Appl. Catal. A, 569 (2019) 141-148.
[22] Y.S. Ryou, J. Lee, S.J. Cho, H. Lee, C.H. Kim, D.H. Kima, Activation of Pd/SSZ-13 catalyst by hydrothermal aging treatment inpassive NO adsorption performance at low temperature for cold startapplication, Appl. Catal. B, 212 (2017) 140-149.
[23] N. Wang, Q. Sun, R. Bai, X. Li, G. Guo, J. Yu, In Situ Confinement of Ultrasmall Pd Clusters within Nanosized Silicalite-1 Zeolite for Highly Efficient Catalysis of Hydrogen Generation, J. Am. Chem. Soc., 138 (2016) 7484-7487.
[24] Q. Sun, N. Wang, Q. Bing, R. Si, J. Liu, R. Bai, P. Zhang, M. Jia, J. Yu, Subnanometric Hybrid Pd-M(OH)2, M = Ni, Co,Clusters in Zeolites as Highly EfficientNanocatalysts for Hydrogen Generation, Chem, 3 (2017) 477-493.
[25] S. Goel, S.I. Zones, E. Iglesia, Encapsulation of Metal Clusters within MFI via Interzeolite Transformations and Direct Hydrothermal Syntheses and Catalytic Consequences of Their Confinement, J. Am. Chem. Soc., 136 (2014) 15280-15290.
[26] L. Liu, M. Lopez-Haro, C.W. Lopes, C. Li, P. Concepcion, L.-. Simonelli, J.J.C. Calvino, A., Regioselective generation and reactivity control of subnanometric platinum clusters in zeolites for high-temperature catalysis, Nat. Mater., 18 (2019) 866-873.
[27] L. Liu, U. Díaz, R. Arenal, G. Agostini, P. Concepción, A. Corma, Generation of subnanometric platinum with highstability during transformation of a 2D zeolite into 3D, Nat. Mater., 16 (2017) 132-138.
[28] L. Liu, D.N. Zakharov, R. Arenal, P. Concepcion, E.A. Stach, A. Corma, Evolution and stabilization of subnanometric metal species in confined space by in situ TEM, Nat. Commun., 9 (2018) Article number: 574.
[29] G.T. Kokotailo, S.L. Lawton, D.H. Olson, W.M. Meier, Structure of synthetic zeolite ZSM-5, Nature, 272 (1978) 437-438.
[30] M.E. Leonowicz, J.A. Lawton, S.L. Lawton, M.K. Rubin, MCM-22: A Molecular Sieve with Two Independent Multidimensional Channel Systems, Science, 264 (1994) 1910-1913.
[31] A. Corma, V. Fornes, S.B. Pergher, T.L.M. Maesen, J.G. Buglass, Delaminated zeolite precursors as selective acidic catalysts, Nature, 396 (1998) 353-356.
[32] A. Corma, V. Fornés, J.M. Guil, S. Pergher, T.L.M. Maesen, J.G. Buglass, Preparation, characterisation and catalytic activity of ITQ-2, a delaminated zeolite, Micropor. Mesopor. Mater., 38 (2000) 301-309.
[33] M. Rutkowska, U. Díaz, A.E. Palomares, L. Chmielarz, Cu and Fe modified derivatives of 2D MWW-type zeolites (MCM-22, ITQ-2 and MCM-36) as new catalysts for DeNOx process, Appl. Catal. B, 168-169 (2015) 531-539.
[34] V.J. Margarit, M.E. Martínez-Armero, M.T. Navarro, C. Martínez, A. Corma, Direct Dual-Template Synthesis of MWW Zeolite Monolayers, Angew. Chem. Int. Ed., 54 (2015) 13724-13728.

[35] H.Y. Luo, V.K. Michaelis, S. Hodges, R.G. Griffin, Y. Román-Leshkov, One-pot synthesis of MWW zeolite nanosheets using a rationally designed organic structure-directing agent, Chem. Sci., 6 (2015) 6320-6324.
[36] E.M. Gallego, C. Paris, C. Martínez, M. Moliner, A. Corma, Nanosized MCM-22 zeolite using simple non-surfactant organic growth modifiers: synthesis and catalytic applications, Chem. Commun., 54 (2018) 9989-9992.
[37] E.M. Gallego-Sanchez, C.G. Paris-Carrizo, M.C. Martinez-Sanchez, M. Moliner-Marin, A. Corma-Canos, Method for synthesising MWW material in its nanocrystalline form and its use in catalytic applications, WO2020025846, (2020).
[38] A. Corma, C. Corell, J. Pérez-Pariente, Synthesis and characterization of the MCM-22 zeolite, Zeolites, 15 (1995) 2-8.
[39] M.D. Argyle, C.H. Bartholomew, Heterogeneous Catalyst Deactivation and Regeneration: A Review, Catalysts, 5 (2015) 145-269.
[40] J. Chen, T. Liang, J. Li, S. Wang, Z. Qin, P. Wang, L. Huang, W. Fan, J. Wang, Regulation of Framework Aluminum Siting and Acid Distribution in H-MCM-22 by Boron Incorporation and Its Effect on the Catalytic Performance in Methanol to Hydrocarbons, ACS Catal., 6 (2016) 2299-2313.